

Experimental Verification of Constitutive Equations for Plasticity Under Biaxial, Cyclic and Non-Radial Loading Conditions

G.T.M. Janssen

*TNO, Institute for Mechanical Constructions,
P.O. Box 29, NL-2600 AA Delft, The Netherlands*

J. Huetink

*Twente University of Technology,
P.O. Box 217, NL-7500 AE Enschede, The Netherlands*

SUMMARY

This paper presents theoretical and experimental results of plasticity research on the austenitic steel WN 1.4948 and the ferritic steel WN 1.6770 both at room temperature. The plasticity experiments have been initiated to arrive at sufficiently accurate and experimentally verified constitutive equations for plastic deformations arising from arbitrary loading histories and for the materials mentioned before. The accurate determination of plastic strains is extremely important for the assessment of the structural integrity of nuclear components.

The description of the plastic deformations has been based on the so-called fraction model of BESSELING sometimes also indicated as sublayer or overlay model. The classical theories show defectives especially for cyclic and non-radial load histories and it did not appear profitable to try to extend the classical theory. However, the multi-yield surface models, which also includes the BESSELING-model, definitely have prospects for further developments.

In the fraction model a volume element is thought to be subdivided into a set of parallel fractions having equal values of total strain. In the most general case each fraction exhibits plasticity and creep properties including (saturating) isotropic strainhardening but the material parameters such as the yield stress and creep-law parameters are different for each volume fraction. Anisotropic hardening is introduced by the interaction of the volume fractions causing a self-balancing system of initial stresses.

The verification of the mathematical description has been performed for biaxial states of stress. General biaxial states of stress can be obtained with thinwalled tubes loaded in a combination of tension, torsion and internal pressure. The whole range of principal stress ratios $-1 < \sigma_1/\sigma_2 < 1$ is covered. About 30 experiments have been performed on the austenitic steel and about 15 experiments on the ferritic steel. Besides loading programmes with monotonically increasing loading conditions also cyclic and non-radial loading histories were considered.

Since the austenitic steel shows considerable strain rate effects at ambient temperature it is found to be necessary to extend the description with viscoplasticity using the BINGHAM-model.

1. Introduction

This paper presents theoretical and experimental results of plasticity research on the austenitic steel X6 CrNi 18 11 and the niobium stabilized ferritic steel 8 CrMoNiNb 9 10 in the German standards indicated as respectively WN 1.4948 and WN 1.6770. This research has been carried out within the framework of a TNO-research programme on inelastic analysis of structural components of the SNR-300.

The plasticity experiments have been initiated to arrive at sufficiently accurate and experimentally verified constitutive equations for plastic deformation arising from arbitrary multiaxial loading histories and for the materials mentioned before. The accurate determination of plastic strain is of importance for the assessment of structural integrity of nuclear components.

The description of plastic deformation has been based on the so-called fraction model of BESSELING [1] sometimes also indicated as sublayer or overlay model. The classical theories show defectives especially for cyclic and non-radial load histories. However, multi-yield surface models such as the BESSELING-model and the MRÓZ-model [2] definitely have prospects for further development.

In the BESSELING-model an infinitesimal volume element is thought to be subdivided into a finite number of parallel fractions. These volume fractions possess different properties with respect to time-independent plastic deformation and/or creep. At volume-fraction level only isotropic hardening rules are used. Anisotropic hardening is introduced by the interaction of the volume fractions causing a self-balancing system of internal stresses.

In this paper, the fraction model has been extended for saturating isotropic hardening and strain rate dependent plastic deformation using the BINGHAM-model [3]. The verification of the mathematical description has been performed for biaxial states of stress. General biaxial states of stress can be obtained with thinwalled tubular specimens loaded in a combination of tension, torsion and internal pressure. In that case the whole range of principal stress ratios $-1 < \sigma_1/\sigma_2 < 1$ is covered. Thirty-two biaxial plasticity experiments with suitable chosen loading programmes have been carried out on the austenitic steel and fourteen on the ferritic steel. All the experiments were carried out at room temperature.

2. Analysis

Figure 1 shows a uniaxial presentation of a fraction model for time-independent plastic deformation. When the volume fractions describe a perfect-plastic material then the fraction model gives a piecewise linear representation (Fig. 2). After a load reversal the BAUSCHINGER-effect is approximated. In order to describe the hardening behaviour such as is observed in the austenitic steel (Fig. 9), also (cyclic strain range dependent) saturating isotropic hardening has to be incorporated in the model.

The experimental evidence that the stress-strain curves for different strain rates are equidistant in fully plastic range (Fig. 3) and the fact that time-dependency was not observed in the elastic range can be modelled by placing a BINGHAM-fraction parallel to the elastic-plastic fractions as is indicated in Figure 5.

Now we will discuss the mathematical description. Firstly, we form the equations of a BINGHAM-fraction. The equations of the time-independent fractions can easily be derived then from the BINGHAM-equations for they are a special case of these equations.

The total deformation rate in a volume fraction k is characterized by the total strain

rate $\dot{\varepsilon}_{ij}$, which is the same for all volume fractions. In each fraction the total strain is subdivided into an elastic and a viscoplastic part:

$$\dot{\varepsilon}_{ij} = \varepsilon_{ij}^{ek} + \dot{\varepsilon}_{ij}^{vk} \quad (1)$$

With HOOKE's law the stress-strain relation for fraction k can be written as:

$$\dot{\sigma}_{ij}^k = E_{ijmn} \dot{\varepsilon}_{mn}^{ek} = E_{ijmn} [\dot{\varepsilon}_{mn} - \dot{\varepsilon}_{mn}^{vk}] \quad (2)$$

where E_{ijmn} is the tensor of elastic constants and is equal for all fractions. Moreover the summation convention with respect to the subscripts is applied.

The total stress rate $\dot{\sigma}_{ij}$ is obtained by summation of the stress rates $\dot{\sigma}_{ij}^k$ over the fractions taking into account the relative volume fraction ψ^k :

$$\dot{\sigma}_{ij} = \sum_{k=1}^N \psi^k \dot{\sigma}_{ij}^k, \quad \sum_{k=1}^N \psi^k = 1 \quad (3)$$

where N is the total number of fractions. Viscoplastic strain rates in fraction k can occur if the stress point is outside or on the yield surface in stress space:

$$\phi^k > 0 \quad (4)$$

During viscoplastic deformation the viscoplastic strain rate is considered to be perpendicular to the yield surface ϕ^k [4] as well as to surface of constant energy dissipation r^k [5]. These conditions can be summarized as:

$$\dot{\varepsilon}_{ij}^{vk} = \dot{\varepsilon}^{ck} \frac{\partial \bar{\sigma}^k}{\partial \sigma_{ij}^k} = \dot{\varepsilon}^{pk} \frac{\partial \bar{\sigma}^k}{\partial \sigma_{ij}^k} \quad (5)$$

where $\bar{\sigma}^k$ must be a homogeneous function of the first degree of the stress components.

The equivalent creep strain rate $\dot{\varepsilon}^{ck}$, equal to the equivalent plastic strain rate, is a function of the equivalent stress in the dashpot (Fig. 5) $\bar{\sigma}^{ck} = \bar{\sigma} - \bar{\sigma}^{Yk}$ where $\bar{\sigma}^{Yk}$ is the uniaxial equivalent yield stress.

Substitution of (5) into (2) and (3) delivers a differential equation for the present model. In incremental form it reads:

$$E_{ijmn} \Delta \varepsilon_{mn} = \Delta \sigma_{ij} + \sum_{k=1}^N \psi^k E_{ijmn} \Delta \bar{\varepsilon}^{ck} \frac{\partial \bar{\sigma}^k}{\partial \sigma_{mn}^k} \quad (6)$$

These equations can be solved by following the general numerical methods for creep analysis. For sufficiently small time steps and isothermal load histories $\Delta \bar{\varepsilon}^{ck}$ can be approximated by $\bar{\varepsilon}_0^c \Delta t$, where $\bar{\varepsilon}_0^c$ is the known creep strain rate at the beginning of time step Δt .

An often more economical procedure is to solve the equations with the tangential-stiffness method. To arrive at these equations HUETINK's numerical method [6] for creep calculation is applied. In this method the severe stress dependency of $\bar{\varepsilon}^{ck}$ has been taken into account by the first order term of TAYLOR's series:

$$\dot{\varepsilon}^{ck} (t_0 + \Delta t) = \dot{\varepsilon}^{ck} (t_0) + \frac{\dot{\varepsilon}^{ck}}{\dot{\sigma}^{ck}} \dot{\sigma}^{ck} \Delta t + 0 (\dot{\sigma}^{ck} \Delta t)^2 \quad (7)$$

By neglecting the second and higher order terms the increment of equivalent creep strain can be written as:

$$\Delta \bar{\varepsilon}^{ck} = \int_{t_0}^{t_0 + \Delta t} \dot{\varepsilon}^{ck} dt = \Delta \bar{\varepsilon}^{cok} + a^k \Delta \bar{\sigma}^{ck} \quad (8)$$

where

$$\Delta \bar{\varepsilon}^{cok} = \dot{\varepsilon}^{ck} (t_0) \Delta t, \quad a^k = \frac{1}{2} \left(\frac{\partial \dot{\varepsilon}^{ck}}{\partial \dot{\sigma}^{ck}} \right)_{t_0} \Delta t$$

The unknown quantity $\Delta \bar{\sigma}^{ck}$ can be eliminated using (2), (8) and the condition that

$$\Delta \bar{\sigma}^{ck} = \Delta \bar{\sigma}^k - \Delta \bar{\sigma}^{Yk} = \frac{\partial \bar{\sigma}^k}{\partial \sigma_{ij}^k} \Delta \sigma_{ij}^k - \frac{\partial \bar{\sigma}^{Yk}}{\partial \bar{\varepsilon}^{pk}} \Delta \bar{\varepsilon}^{pk} = \frac{\partial \bar{\sigma}^k}{\partial \sigma_{ij}^k} \Delta \sigma_{ij}^k - E^{tk} \Delta \bar{\varepsilon}^{pk} \quad (9)$$

where E^{tk} is the tangential modulus which is considered to be constant during the time step Δt .

The resulting incremental equations for a BINGHAM-fraction are:

$$\Delta \sigma_{ij}^k = [E_{ijmn}^k - (1-h^k) Y_{ijmn}^k] [\Delta \varepsilon_{mn}^k - h^{ck} \Delta \bar{\varepsilon}^{cok} \frac{\partial \bar{\sigma}^k}{\partial \sigma_{mn}^k}] \quad (10)$$

where

$$Y_{ijmn}^k = (E_{ijpg}^k \frac{\partial \bar{\sigma}^k}{\partial \sigma_{pg}^k} \frac{\partial \bar{\sigma}^k}{\partial \sigma_{rs}^k} E_{rsmn}^k) / B^k, \quad B^k = \frac{\partial \bar{\sigma}^k}{\partial \sigma_{ij}^k} E_{ijmn}^k \frac{\partial \bar{\sigma}^k}{\partial \sigma_{mn}^k}$$

$$h^k = \frac{1 + a^k E^{tk}}{1 + a^k B^k + a^k E^{tk}}, \quad h^{ck} = \frac{1}{1 + a^k E^{tk}}$$

For pure creep the following equations hold:

$$h^k = \frac{1}{1 + a^k B^k} \quad \text{and} \quad h^{ck} = 1 \quad (11)$$

and for time-independent plasticity

$$h^k = \frac{E^{tk}}{E^{tk} + B^k} \quad \text{and} \quad h^{ck} = 0 \quad (12)$$

In the material model shown in Figure 5 the first fraction is a BINGHAM-fraction and the other fractions are time-independent elastic-plastic fractions. Summation over N volume fractions yields:

$$[E_{ijmn}^k - \sum_{k=1}^N \psi^k (1-h^k) Y_{ijmn}^k] \Delta \varepsilon_{mn}^k =$$

$$\Delta \sigma_{ij}^k + \psi^1 [E_{ijmn}^1 - (1-h^1) Y_{ijmn}^1] h^{c1} \Delta \bar{\varepsilon}^{c01} \frac{\partial \bar{\sigma}^1}{\partial \sigma_{mn}^1} \quad (13)$$

3. Determination of model parameters

In the present description we adopted the following starting points. The yield surface of volume fraction k is based on the yield criterion according to VON MISES:

$$\phi^k = \frac{1}{2} s_{ij}^k s_{ij}^k - \frac{1}{3} (\bar{\sigma}^{Yk})^2 = \frac{1}{3} (\bar{\sigma}^k)^2 - \frac{1}{3} (\bar{\sigma}^{Yk})^2 = 0 \quad (14)$$

where s_{ij} is the deviatoric stress tensor.

The yield stress $\bar{\sigma}^{Yk}$ is considered to be a function of the accumulated plastic strain $\bar{\epsilon}^{pk}$ in the following way:

$$\bar{\sigma}^{Yk} = \bar{\sigma}_0^{Yk} + \sum_{i=1}^M \Delta \sigma_1^{Yk} \left\{ 1 - \exp \left(-\frac{\bar{\epsilon}^{pk}}{\bar{\epsilon}_{oi}} \right) \right\}, \quad M = 1 \text{ or } 2 \quad (15)$$

where

$$\bar{\epsilon}^{pk} = \int_0^t \left(\frac{2}{3} \dot{\epsilon}_{ij}^{pk} \dot{\epsilon}_{ij}^{pk} \right)^{\frac{1}{2}} dt$$

For the description of the strain rate effects we introduced in the first fraction the following creep energy dissipation function for secondary creep:

$$f^1 = A^1 \left(\frac{\bar{\sigma}_0^{-1} - \bar{\sigma}^{Y1}}{\bar{\sigma}_0^{-1}} \right)^{2n^1} = (\bar{\sigma}^{-1} - \bar{\sigma}^{Y1})^{\frac{2}{3}} \bar{\epsilon}^{c0} \quad (16)$$

The stress $\bar{\sigma}_0^{-1}$ is introduced to obtain a dimensionless quantity between the brackets, $\bar{\sigma}^{Y1}$ is the current yield stress and $\bar{\sigma}^{-1}$ is the equivalent stress according to VON MISES.

The viscoplastic parameters that are to be determined experimentally are ψ^1 , n^1 , A^1 and $\bar{\sigma}_0^{-1}$. They can be determined from a number of tension or torsion tests with different but constant strain rates (Fig. 3) and a test with relaxation periods (Fig. 4). The size of the viscoplastic fraction may be derived from the slopes just before and after a relaxation period (Fig. 4). The isotropic hardening parameters can be derived from a cyclic tension or torsion test with a sufficiently large strain range as is shown in Figure 9. From this figure the values $\Delta \bar{\sigma}_i^{-Y}$ and $\bar{\epsilon}_{oi}^{-}$ can be obtained. The corresponding parameters of fraction k are assumed to be :

$$\Delta \bar{\sigma}_i^{-Yk} = \frac{\bar{\sigma}_0^{-Yk}}{\bar{\sigma}_0^{-Y}} \Delta \bar{\sigma}_i^{-Y}, \quad \bar{\epsilon}_{oi}^k = \bar{\epsilon}_{oi}^{-}, \quad i = 1 \text{ or } 2 \quad (17)$$

where

$$\bar{\sigma}_0^{-Y} = \sum_{k=1}^N \psi^k \bar{\sigma}_0^{-Yk}$$

The parameters ψ^k and $\bar{\sigma}_0^{-Yk}$ can be derived from the so-called static deviatoric stress-strain curve which is approximated by a number of straight lines as is indicated in Figure 7. The static stress-strain curve is approximated by subtracting the asymptotic value $s_{xx}^{co} = \frac{2}{3} \sigma_{xx}^{co}$ from the total stress-strain curve. The slope of the several straight lines determine the volume fractions ψ^k . The initial yield stresses $\bar{\sigma}_0^{-Yk}$ follow directly from the strain at the

breakpoints. The parameter h_{qm}^k is according to (12) and is the mean value between the breakpoints q and $q+1$. The resulting model parameters of the materials considered are collected in Table 1.

4. Experimental verification of the model

Figure 8 shows the tubular specimens used for the biaxial plasticity experiments. The axial strain and the shear deformation in the specimens of austenitic steel were measured with special developed extensometers and gauge-rings with sliding contacts. The circumferential strain was measured with 4 high-strain strain gauges [7]. In the ferritic tubular specimen all strains were measured with strain gauges. The axial load and the twisting moment were measured with a load cell, and the internal pressure with an electronic pressure gauge.

Thirty-two experiments were carried out on the austenitic steel WN 1.4948 and analysed with present model (Fig. 5). Some provisional results were already reported in [8]. Three experiments were performed on artificially aged material. This ageing was carried out under a tensile stress of 112.3N/mm^2 at 600°C during 50 hours. A small number of experiments were used for parameter determination (Table 1). Loadhistories with and without loadreversals were considered and also experiments under non-radial load conditions. Some examples of a comparison of theoretical and experimental results are shown in the Figures 9-12. The results shown in Figure 12 concern artificially aged material.

Fourteen experiments were carried out in the ferritic steel WN 1.6770 and were analysed with the model shown in Figure 1. Also here a small number of experiments were used for parameter determination (Table 1). Some theoretical and experimental results of this material are shown in the Figures 13 and 14.

5. Conclusions

Both for the austenitic steel WN 1.4948 and for the ferritic steel WN 1.6770 the plastic deformation can be predicted quite satisfactory. The description of the strain rate effects observed in the austenitic steel is also quite satisfactory. For the ferritic steel this effect was omitted because it was far less pronounced than for the austenitic steel. Also a quite accurate description is given of saturating isotropic strainhardening where isotropic hardening is considered to be a function of accumulated plastic strain.

The description of the gradual transition from elastic to fully plastic behaviour after one or more loadreversals still calls for improvement. Especially for non-radial loadconditions this can lead to differences between theoretical and experimental results. Special attention has to be paid to the distribution of isotropic hardening over the fractions. It might be possible that introduction of softening cannot be avoided.

The accuracy of the prediction of artificially aged material is comparable with the predictions for the material in as delivered condition. Adaption of the model is not necessary only the parameters have to be determined again.

Acknowledgement

This work was commissioned by the Project Group of Nuclear Energy TNO. The authors thank the Project Group and the Dutch Ministry of Economic Affairs for the permission to publish this paper. The authors are also grateful to Prof. J.F. BESSELING and Prof. P. MEIJERS for their valuable advice and to all other collaborators of this project.

References

- [1] BESSELING, J.F., "A theory of elastic, plastic and creep deformation of an initially isotropic material showing anisotropic strain-hardening, creep, recovery and secondary creep," J. Appl. Mech., 25, 529-536, (1953).
- [2] MRÓZ, Z., "On the description of anisotropic workhardening," J. Mech. Phys. Solids, 15, 163-175, (1967).
- [3] BINGHAM, E.C., "Fluidity and Plasticity (Chapter VIII, 215-218)", McGraw-Hill. (1922).
- [4] DRUCKER, D.C., "A more fundamental approach to plastic stress-strain relations," Proc. First USA National Congr. Appl. Mech., 487-491, (1951).
- [5] ZIEGLER, H., "Zwei Extremalprinzipien der irreversiblen Thermodynamik", Ingenieur Archive, 30, 410-416, (1961).
- [6] HUETINK, J., Numerical method for creepcalculations with adaption of the stiffnessmatrix (in Dutch)," TNO-IWECO, Report No. 5011009-79-1, (1979).
- [7] BOOIJ, J. and VAN DER WERFF, K., "A description of plasticity experiments on austenitic stainless steel tubes". Delft University of Technology, WTHD no. 77, (1975).
- [8] MEIJERS, P., JANSSEN, G.T.M. and BOOIJ, J., "Numerical plasticity and creep analysis based on the fraction model and experimental verification for AISI 304". SMIRT III, Paper L 3/9, LONDON (1975).

TABLE 1. MODEL PARAMETERS

Material	WN 1.4948		WN 1.4948 artificially aged		WN 1.6770	
E [N/mm ²]	191000.		202000.		188000.	
ν	0.28		0.28		0.28	
$\psi^1 \frac{\bar{\sigma}_o^Y}{\sigma_o^Y}^1$ [N/mm ²]	0.7364	84.6	0.7483	129.9	0.4295	206.6
$\psi^2 \frac{\bar{\sigma}_o^Y}{\sigma_o^Y}^2$ -	0.2193	212.6	0.2081	314.3	0.3833	406.6
$\psi^3 \frac{\bar{\sigma}_o^Y}{\sigma_o^Y}^3$ -	0.0363	637.9	0.0301	683.4	0.1156	703.7
$\psi^4 \frac{\bar{\sigma}_o^Y}{\sigma_o^Y}^4$ -	0.0078	1343.0	0.0078	1640.0	0.0572	1135.1
$\psi^5 \frac{\bar{\sigma}_o^Y}{\sigma_o^Y}^5$ -	0.0002	REMAINS ELASTIC	0.0057	REMAINS ELASTIC	0.01447	REMAINS ELASTIC
A^1 [N/(mm ² .s)]	0.04866		12.73			
$\bar{\sigma}_o^1$ [N/mm ²]	84.6		129.9			
n^1	4		4			
$\Delta \frac{\bar{\sigma}_1^Y}{\sigma_1^Y}$ [N/mm ²] $\bar{\epsilon}_{01}$	27.7	0.005	159.3	0.165	90.8	0.025
$\Delta \frac{\bar{\sigma}_2^Y}{\sigma_2^Y}$ - $\bar{\epsilon}_{02}$	190.5	0.135				

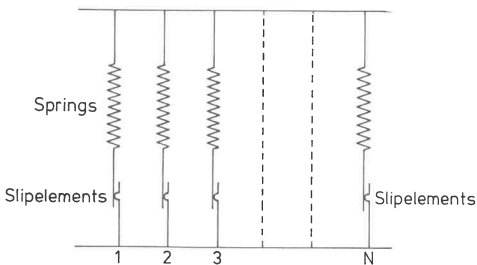


Fig. 1 Model for time-independent plastic deformation

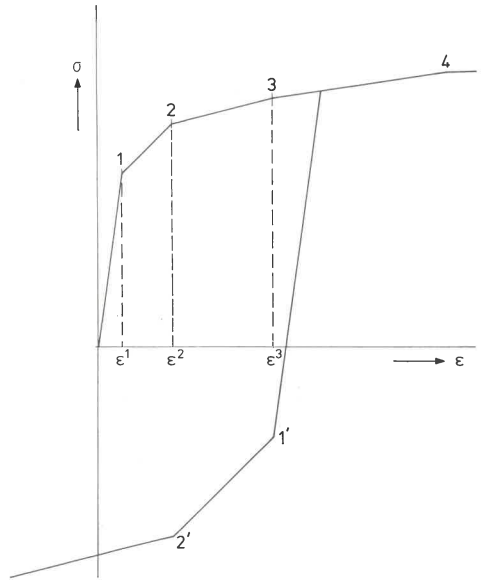


Fig. 2 Multi-linear representation of a stress-strain curve (4 volume fractions)

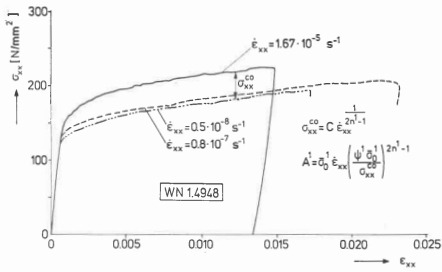


Fig. 3 Strain rate effect for WN 1.4948

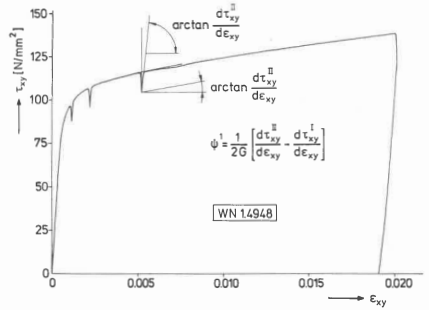


Fig. 4 Torsion curve with relaxation periods (900 s)

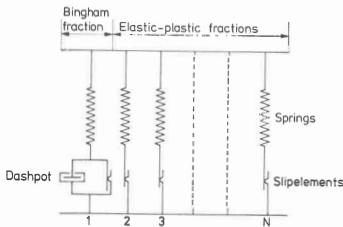


Fig. 5 Modified model for time-dependent plastic deformation

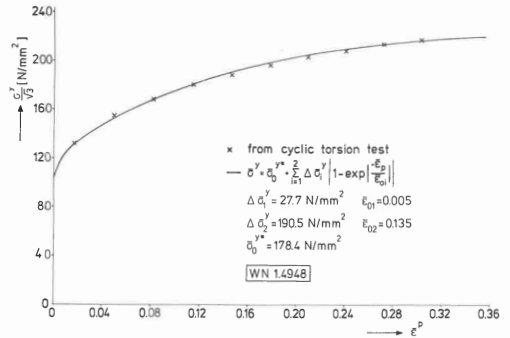


Fig. 6 Saturating isotropic strain hardening

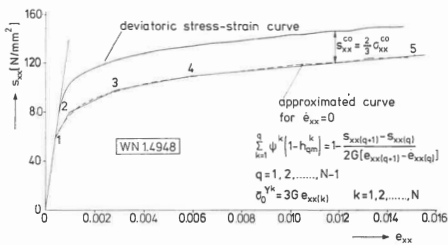


Fig. 7 Approximation of a deviatoric stress-strain curve for $\dot{\epsilon}_{xx} \rightarrow 0$

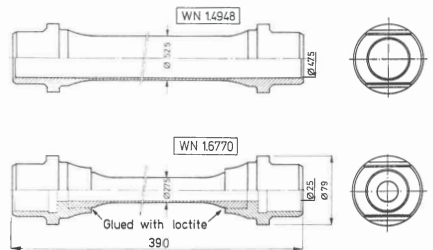


Fig. 8 Tubular specimens for plasticity experiments

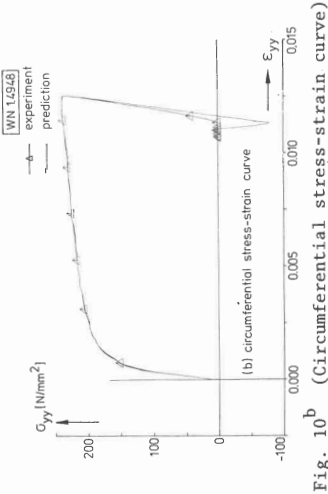


Fig. 10^b (Circumferential stress-strain curve)

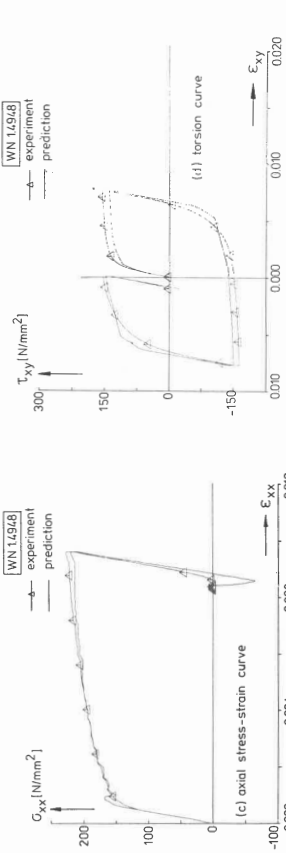


Fig. 10 Tension and internal pressure simultaneously applied followed by a torsion cycle

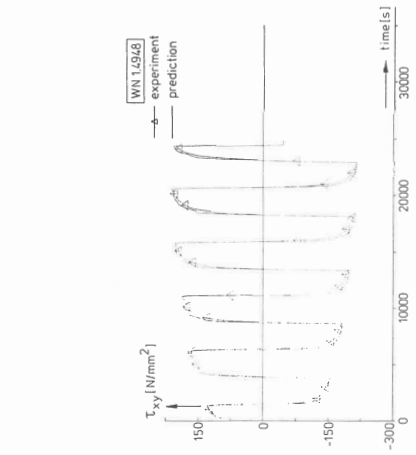


Fig. 9 Cyclic torsion

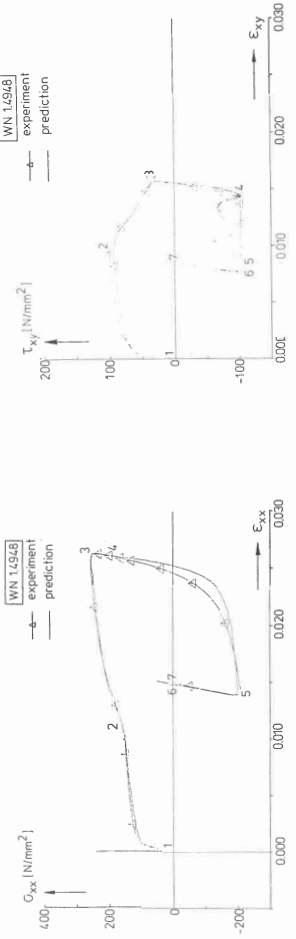
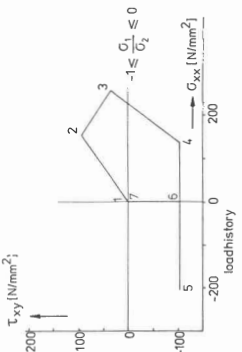


Fig. 11 Non-radial load history in a combination of axial load and torsion



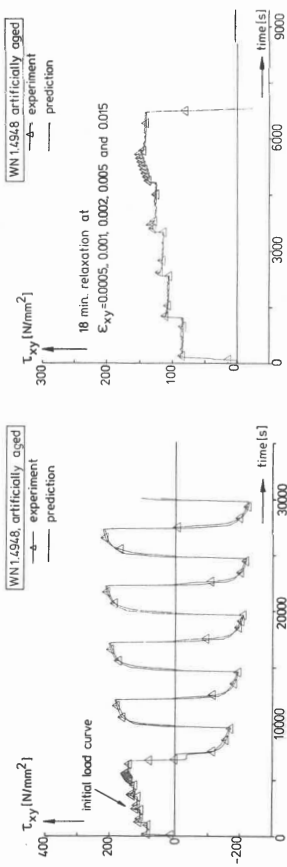


Fig. 12 Cyclic torsion with relaxation periods in the initial load curve

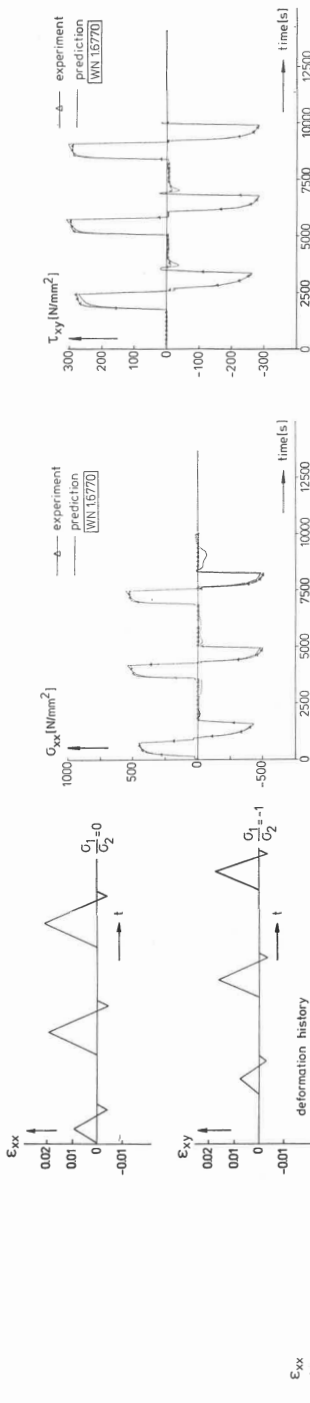


Fig. 13 Cyclic axial load and cyclic torsion alternately applied

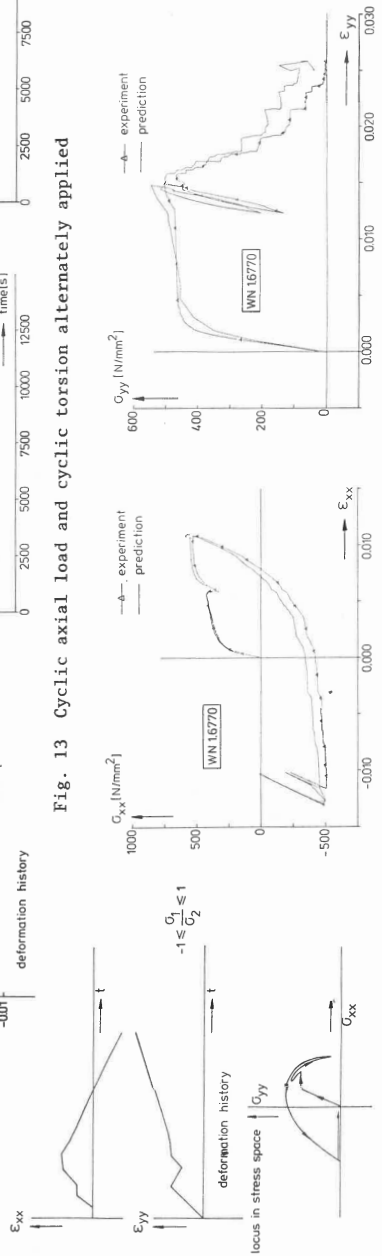


Fig. 14 Non-radial load history in a combination of axial load and internal pressure

